

LABORATORY STUDY ON TRANSPORT OF CORAL GRAVELS UNDER FORWARD-LEANING NEARSHORE WAVES

Yoshimitsu Tajima¹ and Shota Seto¹

Abstract

This study focuses on behavior of coral gravels under forward leaning waves around the surf and swash zones. We first carried out laboratory experiments in which regular periodic waves were normally incident on coral gravel bed with grain size of around 1cm. Waves, currents and moving gravels were captured through the analysis of video images recorded from the side of the flume. Besides water surface fluctuations and near-bottom current velocities, moving gravels were extracted by detecting abruptly changing brightness of succeeding two images and locations and velocities of these moving gravels were recorded. It was found through comparisons of these time-varying quantities of water surface fluctuations and velocities of moving gravels and surrounding currents that the acceleration of near-bottom fluid has significant influence on movement of coral gravels.

Key words: coral gravels, forward-leaning waves, surf zone, swash zone, morphodynamics of coral beach, laboratory experiments, porous bed

1. Introduction

Understanding physical mechanisms of formation of coral cay is one of key tasks for designing and planning appropriate protection and conservation strategies of coral coasts. Ballast island, for example, is a small coral cay on the isolated coral reef located offshore of Iriomote-jima island in Okinawa, Japan and this small island with the width of just several meters, the length of around thirty meters and the height of a couple of meters above the mean sea level, has been kept formed on the reef for more than fifty years although waves and currents on the reef have often changed the shape and locations of the island (Kayanne et al., 2016). Mechanisms of such natural formation process of coral cays can be applied to sustainable coastal protection measures.

Authors carried out a field survey focusing on such natural processes of formation of Ballast island and pointed out through comparisons of numerical analysis and observed features that wave-associated transport of coral gravels plays dominant role to form the coral cay (Takemori et al., 2015). This study focuses on behavior of coral gravels especially under waves in the shallow water. Shoaling waves may be breaking, broken and running up on a porous gravel bed and the transport of coral gravels may be affected by forward-leaning profiles of wave orbital velocity. To capture such characteristics, this study first carries out laboratory experiments using coral gravels and quantifies the behavior of each gravel and surrounding hydrodynamics through applications of image-based analysis.

2. Laboratory Experiments

To capture the behavior of coral gravels under waves, this study first carried out laboratory experiments, in which regular periodic waves were incident on actual coral bed placed in the wave flume. The first experiment A mainly focused on formation of coral cays and the second experiment B focuses more on the movement of coral gravels on different bed slopes.

¹Dept. of Civil Eng., School of Eng., The University of Tokyo, Japan. yoshitaji@coastal.t.u-tokyo.ac.jp

2.1. Setups of the experiment

Figures 1 and 2 respectively show setups of laboratory experiments A and B with examples of recorded pictures. The experiment A, Figure 1, focuses mainly on formation of equilibrium profile of coral bed (Fujikawa and Tajima, 2016) but behavior of moving gravels and fluctuating water surface profiles were also captured through image-based analysis. The experiment B, on the other hand, focuses more on the characteristics of wave-induced movement of coral gravels and only five regular periodic waves were incident on uniformly sloping bed.

In both experiments, coral gravels with diameter of around 1cm, as shown in Figure 1, were placed on the plane fixed bottom of the wave flume with length of 33m and the width of 60cm. The flume has piston-type wave generator. A straight circular pipe line with bulbs and a pump connects both ends of the flume to generate circulating current flow in the flume. The water in the flume was colored in blue and the one side wall of the flume was colored in yellow. Fluctuating water surface and moving gravels were captured from the outside of the other side of the glass wall of the flume by video cameras with frame rate of 30fps and 60fps respectively in the experiment A and B.

In the experiment A, either regular periodic waves or random waves were incident until the coral bed forms equilibrium profile. To represent a coral cay on isolated coral reef, all the bulbs were kept open so that the mean water levels on both sides of the flume balance with each other.

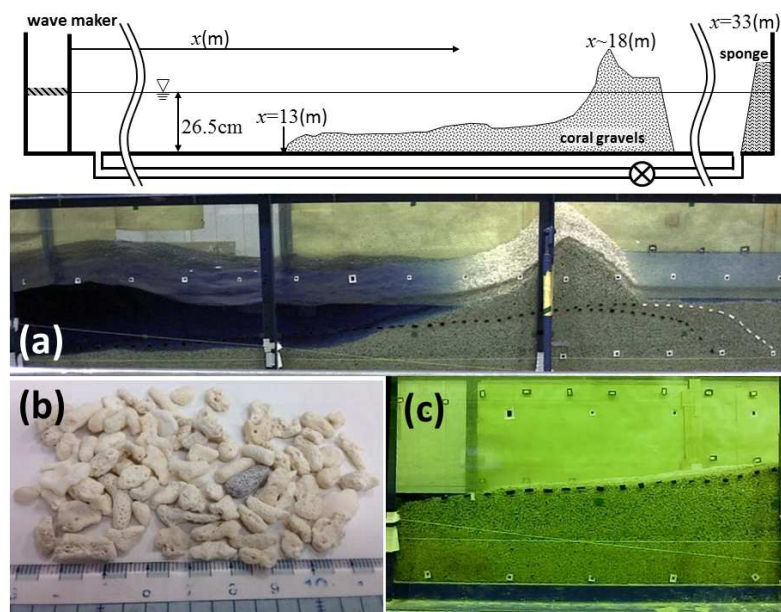


Figure 1. Setups of the experiment A. Examples of (a) recorded image, (b) coral gravels, and (c) rectified image.

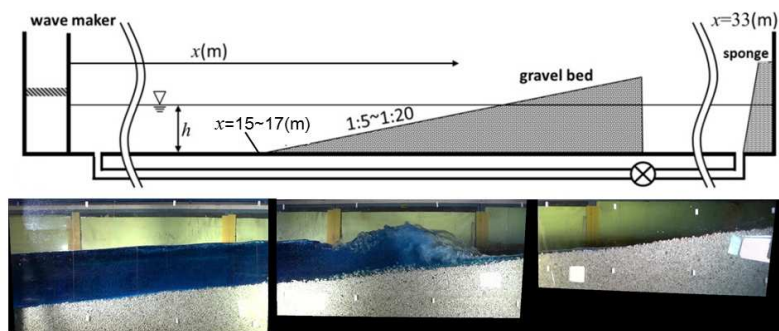


Figure 2. Setups of the experiment B and an example of rectified image.

The experiment B, on the other hand, focuses on the first five periodic regular waves and all the bulbs were closed. Plane coral bed with uniform slope of either 1/5 or 1/10 was formed in each experimental case with offshore constant water depth of $h=42\text{cm}$ and repeatability of wave characteristics and moving gravels were confirmed by repeating the same experiment for three times. Tracer particles with diameter of 0.35mm and specific density of around unity were also put into the water to apply PIV discussed in the next section. Stream function method (Dean, 1965) was applied for determination of incident wave signal of the piston type wave generator so that the generated waves well represent non-linear skewed profile at the wave generator.

2.2. Image-Analysis

This section outlines procedures of various image-based analysis for quantitative estimations of water surface fluctuations, current velocities and moving gravels.

2.2.1. Image-rectification

Following Tajima et al. (2009), we first rectified the recorded images based on the XY-coordinates on the side glass wall of the flume as shown in Figures 1 and 2. Figure 1(c), for example, shows the rectified image in the range of $16\text{m} < x < 17\text{m}$ with x , onshore distance from the wave generator as indicated in Figure 1(a). Figure 2(c) also shows combined rectified images in the range of $17\text{m} < x < 20\text{m}$. Since these rectified images are based on the plane rectangular coordinate system along the side glass wall, horizontal and vertical displacement or movement of fluid, tracer particles and bed gravels can be directly quantified once the target is specified in these rectified images.

Figure 3, for example, shows time-varying bed profiles extracted from the rectified image of the experiment A when regular periodic waves with period of 3sec were generated. Observed bed profile reached to the equilibrium state around 70 minutes after starting the wave generation. As seen in the Figure, steeper bed slope of around $\tan\beta=2/5\sim 3/5$ was quickly developed around the swash zone while change of the bed slope was relatively minor elsewhere. It can also be deduced from the observed well-developed berm profile behind the swash zone that shoreward transport was dominant in this experimental case.

2.2.2 Extraction of moving gravels

Characteristics of moving gravels were first investigated through the image analysis of the experiment A, as shown in Figure 4. A pair of still images succeeding in time was compared with each other and pixels on moving gravels were extracted by detecting pixels whose brightness increase by more than ten percent from the previous to the next images. Figure 4(a) shows an example of rectified still images obtained from the recorded video image and Figure 4(b) shows distributions of detected pixels on moving gravels. The area of Figure 4(b) corresponds to the dashed rectangular frame shown in Figure 4(a) and only the pixels on moving gravels were shown in black while the others are shown in white.

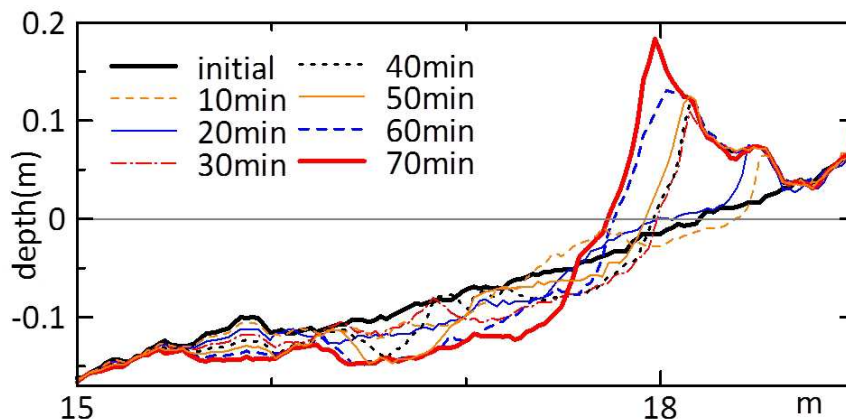


Figure 3. Extracted bed profiles in the experiment A.

Figures 4(c), (d) and (e) then show relationship between moving gravels and wave profiles. Figures 4(c) and 4(e) respectively show time-varying water surface profiles at location A and B indicated in Figure 4(a). Figure 4(c) was created through the following procedures: (i) extract the pixel data along the vertical line at A from each of succeeding images; (ii) place extracted vertical line data of succeeding images side by side in the order of the recorded time of each image. Horizontal axis of Figures 4(c) and (e) therefore indicates the time while the vertical axis of these figures corresponds to the vertical distance. From Figures 4(c) and (e), one can clearly see time-fluctuating water surface boundaries and forward-leaning wave profiles show certain time-gap between (c) and (e). Figure 4(d), on the other hand, was created by the following procedures: (i) extract the pixel data along a straight line from A to B indicated in Figure 4(a) from each succeeding images of Figure 4(b); and (ii) align the extracted line data in the vertical direction and place these line data from each image side by side in the order of recorded time. The horizontal axis of Figure 4(c) therefore corresponds to those of Figures 4(c) and (e), i.e., the time, while the vertical axis of Figure 4(c) indicates the distance along the straight line from A to B.

Since the pixel data in Figure 4(d) was extracted from the images which highlighted only the pixels of moving gravels in black, as shown in Figure 4(b), all clumps of black pixels shown in Figure 4(d) indicate temporal and spatial distributions of moving gravels. As seen in the figure, groups of these clumps, each of which should correspond to the track of identical gravels, aligns in the right downward directions. This feature indicates that each gravel moves mainly in the rightward, i.e., the onshoreward direction under the waves and little offshoreward movement of gravels was observed under this experimental condition. Furthermore, the left end of these series of black clumps indicates the time and location when and where each gravel initiated to move under the wave. Red dashed line in Figure 4(d) shows the timing when the crest of the forward-leaning water surface profile passes each location and, as seen in the figure, many of observed left ends of the group of black clumps are located along the red dashed lines, i.e., many gravels initiate to move in the vicinity of the front face of the forward-leaning water-surface profile.

2.2.3 Velocity of moving gravels

To further investigate the characteristics of moving gravels under the forward-leaning waves, PIV was applied on the series of images of extracted gravels shown in Figure 4(b) with rectangular interrogation

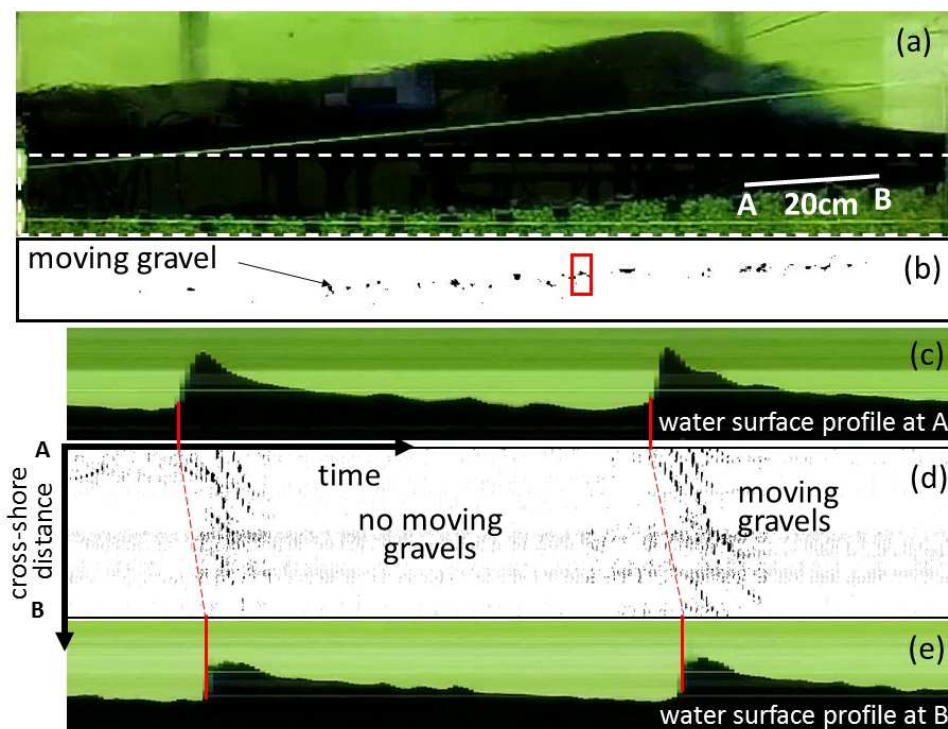


Figure 4. Image analysis of moving gravels in the experiment A: (a) snapshot of rectified image; (b) extracted moving gravels (black pixels); (c) and (e) profiles of water surface at A and B; and (d) temporal and spatial distributions of moving gravels along the line AB shown in (a).

window size of 40 and 20 pixels respectively in the vertical and the horizontal directions, as shown in red solid rectangular in Figure 4(b). The pixel size of rectified images was set to 0.1mm. Velocities of each gravel were extracted from succeeding 6,000 images with the frame rate of 30 fps and obtained velocities were classified into multiple sections at different cross-shore locations and at different phase of incident waves. One-meter-long cross-shore domain was separated into one hundred sections with horizontal intervals of 1cm, and the incident wave were separated into 30 sections. Since the period of incident regular wave was three seconds, the time-interval of each section was 0.1 seconds. The total number of sections, in which obtained velocities of each gravels are classified, is therefore 3,000 as a product of 100 cross-shore sections and 30 sections in phase. Classified velocities in each section were then averaged over after excluding top and bottom 10% of velocities to avoid the influence of noises of estimated velocities.

2.2.4 Water surface fluctuations and wave-induced current velocity

Instantaneous water surface profiles were then extracted from the same succeeding 6,000 images with cross-shore intervals of 1mm. The air-water boundary at each cross-shore location was searched from the pixel under the water to the pixel above the boundary in the vertical upward direction and the boundary was defined by the pixel whose value of $p_1=R+G-B$ with R , G and B , scaled RGB-values of each pixel first exceeds the threshold value. Obtained 6,000 cross-shore profiles were then classified into thirty different phase sections and classified water levels at cross-shore locations and at each phase section were averaged over.

In the experiment B, PIV was applied for quantitative estimations of wave orbital velocity near the bottom. Rectified RGB-images were first converted to gray-scale images based on the parameter, $p_2=B/(R+G+B)$, with pixel size of 0.5mm. Figure 5 shows an example of this conversion. The parameter, p_2 , was defined through trial-and-errors so that obtained gray-scale images yields clear contrast between white tracer particles and the water colored in blue. The interrogation window of PIV was set to 40x40 pixels and horizontal and vertical velocity components were estimated at each of the square grid coordinates with grid intervals of 5mm. It was confirmed that obtained near-bottom horizontal velocity components were nearly uniform in the vertical direction above the bottom boundary layer with thickness of around 2cm. Following discussions therefore just show near-bottom horizontal velocity above the bottom boundary layer.

3. Discussions

This section discusses observed characteristic behavior of coral gravels under the forward-leaning nearshore waves.

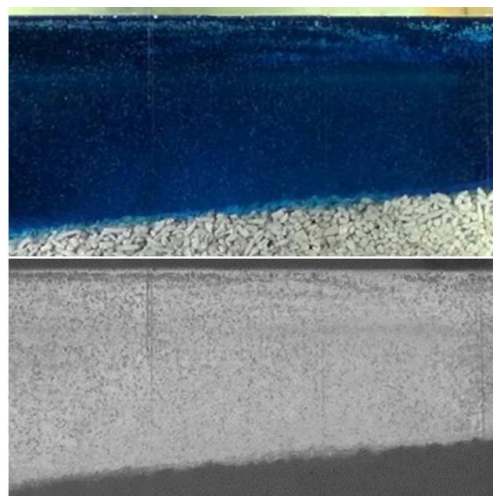


Figure 5. Original image (top) and converted image for PIV (bottom).

3.1. Overall Behavior of Coral Gravels on Quasi-Equilibrium Bed

Figure 6 compares cross-shore distributions of obtained water surface profiles and averaged gravel velocities at each section in the experiment A with incident wave period of 3sec after the coral bed profile nearly reached to the equilibrium state as shown in Figure 3. The figure shows three pairs of panels which compare water surface profiles and velocities of moving gravels respectively at three different phase conditions. In the top panel of each panel, a solid line is the averaged water surface profile and the shaded area indicates the range of maximum and minimum water levels at each cross-shore location. In the bottom panel, on the other hand, vertical bars indicate the averaged gravel velocity at each cross-shore section. No vertical bars were plotted if there was no moving gravels at each cross-shore location. In this experiment no gravels was observed to move offshoreward and thus all the velocities shown in the figure are in the onshoreward direction.

As seen in the Figure, moving gravels, i.e., vertical bars, are found even on the right side, i.e., onshore side, of the front face of the forward-leaning wave profiles in each of three different phase conditions. Averaged velocities of moving gravels under the front face of the waves, moreover, are relatively large compared to those of gravels located in the vicinity of wave crest, where the shoreward horizontal velocity should have at its peak value. This feature may indicate that the magnitude of near-bottom horizontal velocity by itself is not able to fully explain characteristic movement of gravels such as initiation of motion and transporting velocities. This feature may be further supported by the top pair of the figure, in which no moving gravels were found in the vicinity of $x=16\text{m}$, where the water surface level is at its peak. Because of relatively larger water depth around $x=16\text{m}$, the bed appears to be close to the threshold condition of the initiation of motion of coral gravels and thus less number of moving gravels were found in this vicinity. Under this condition, gravels are initiated to move only under the front face of the forward leaning waves but not under the crest.

At the front face of the forward leaning wave profile, the water level is rapidly elevated in time and a large onshoreward pressure gradient force induces a large onshoreward acceleration of the flow. Such large shoreward pressure gradient force may also have nonnegligible influence on behavior of coral gravels. Figure 7 compares distributions of the number and the averaged velocity of observed moving gravels as functions of the instantaneous water level, η , and the time-derivative of the water level, $\partial\eta/\partial t$. All the

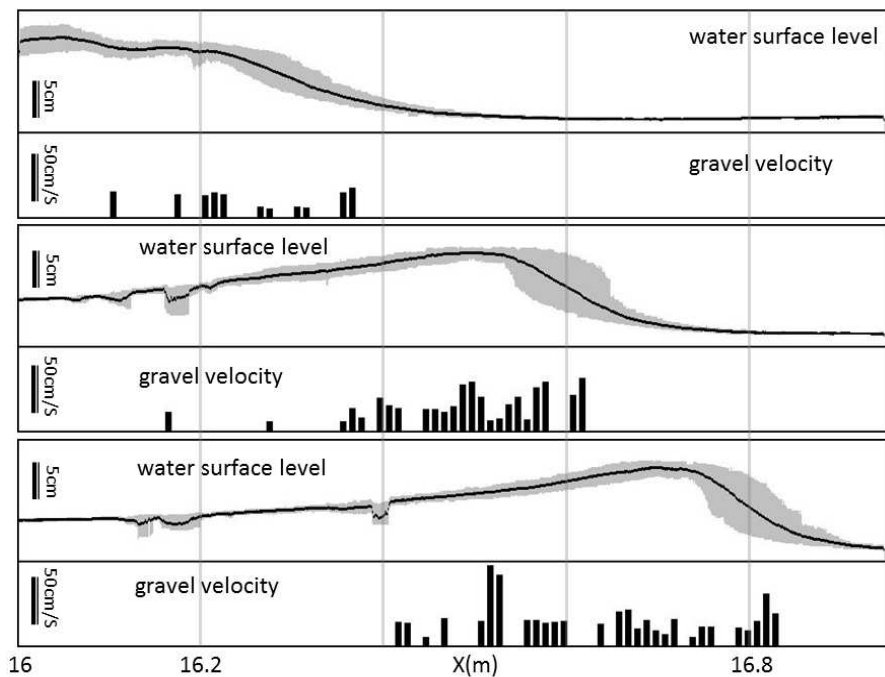


Figure 6. Cross-shore distributions of water surface profiles and shoreward velocities of moving gravels. Solid lines and shaded area indicate averaged and max.-min. range of water surface levels of multiple waves under the same phase condition and vertical bars indicate averaged velocities of moving gravels under waves with the same phase conditions. Three pairs of panels compare those features at different phase conditions.

data used in this figure are based on the same experiment A shown in Figure 6 but include all the phase conditions and all the cross-shore locations within the range of $16\text{m} < x < 17\text{m}$. In Figure 7, horizontal and vertical axes are η and $\partial\eta/\partial t$, respectively, and the color of the map indicates the number of coral gravels, N , passing through each cross-shore location within a unit time (left) and the average velocity of moving gravels (right), respectively. In the figure, the number of moving gravels, N , was scaled by its maximum value, N_{max} . Blank grids in these two figures indicate either of the following three cases: (i) there was no moving gravels; (ii) average velocity of moving gravels were negligibly small; and (iii) there was no data of such combinations of η and $\partial\eta/\partial t$ in this experiment. Black arrows in the figure indicate the circulating direction of time-varying η and $\partial\eta/\partial t$ under the forward leaning waves.

As seen in the figure, the larger numbers of moving gravels tend to concentrate on the right side of the figure, i.e., around the higher η while the relatively larger velocities of moving gravels are distributed around the left top and right top corners of the figure with relatively larger positive $\partial\eta/\partial t$. After the wave crest passes over the gravel, the shoreward velocity of this gravel decreases while the other gravels behind with larger velocity may catch up. This feature reasonably explains how the number of moving gravels increase on the rear-side of the wave crest, as seen in the left panel of Figure 7.

It should also be noted that a certain number of moving gravels were observed under the negative, η , i.e., the water level below the mean water level where the flowing direction of near-bottom wave orbital velocity should be offshoreward. This feature also supports the important impact of $\partial\eta/\partial t$ on behavior of moving gravels.

3.2. Moving Velocity of Gravels on Uniformly Sloping Bed

To further investigate the characteristics of moving gravels under the forward leaning waves with skewed and asymmetric orbital flow velocity, behavior of gravels were analyzed under the first five periodic waves with period of 3sec propagating on uniformly-sloping coral bed in the experiment B. Figure 8 shows temporal and spatial distributions of: (a) water surface level; (b) near-bottom horizontal velocity and (c) acceleration of the flow just above the bottom boundary layer. In the Figure, magnitudes of these variables are indicated in color and vertical and horizontal axes are the time positive in downward direction and cross-shore locations positive in the onshoreward direction, respectively. Blank circles in the figure indicate the track of representative moving gravels. The bed slope conditions of this figure is $\tan\beta=1/10$ and the similar figure in the case of $\tan\beta=1/5$ will be presented and compared with this figure later. Cross-

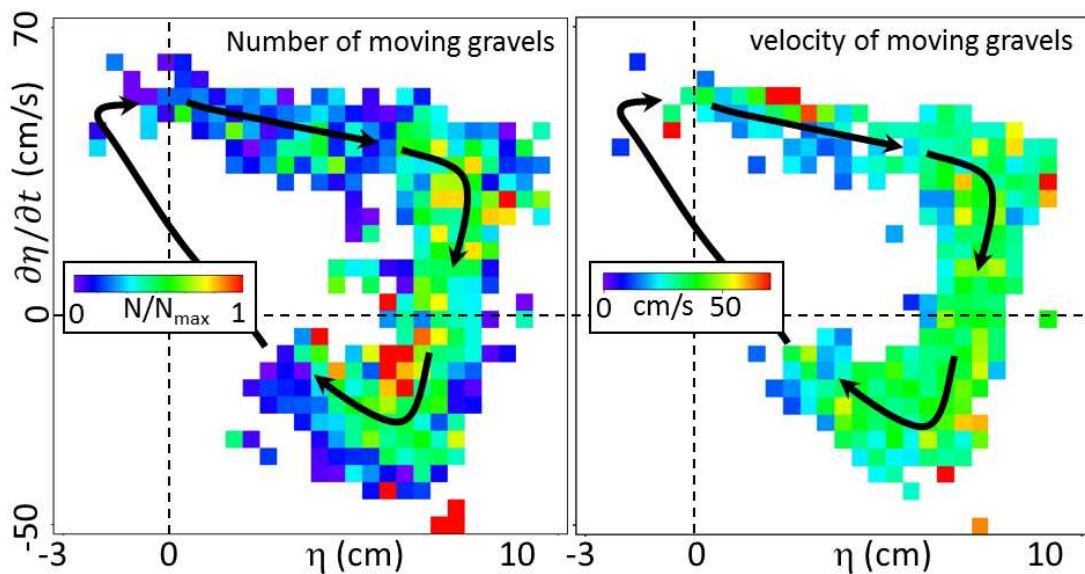


Figure 7. Distributions of the number (left) and the average velocity (right) of moving gravels as functions of instantaneous water level, η , and its time derivative, $\partial\eta/\partial t$.

shore domains of this Figure covers from $x=18\text{m}$ to 19m , which corresponds to the still water depth from 22cm to 12cm . Figure 9 is also based on the same experiment but compares observed velocity of moving gravels with the time profiles of water surface level, horizontal velocity and acceleration of the near-bottom wave orbital velocity at $x=18.5\text{m}$, i.e., in the middle of the cross-shore location shown in Figure 8 with still water depth of 17cm . Series of blank circles in Figure 8 traces the identical gravels and all these tracks extend to the right downward directions, i.e., all the gravels move onshoreward direction and no offshoreward movement was observed in this experimental case. It is also interesting to note that little movement of gravels was observed under the first wave at around $t=3\text{sec}$ while the magnitude of horizontal velocity of the first wave, shown in Figure 9, is nearly equivalent to those of the second and the third waves. The flow acceleration of the first wave, however, is significantly smaller than those of the second and the third waves. This feature also indicates the important impact of the flow acceleration, i.e., horizontal pressure gradient force, on the movement of coral gravels.

Figure 10 shows the same set of panels of Figure 8 but for the case when the same periodic waves with period of 3sec was incident on the plane coral bed with slope of $\tan\beta=1/5$. Horizontal axis also covers 1m -long cross-shore domain with the still water depth from $h=22\text{cm}$ to 2cm . The water depth at the offshore

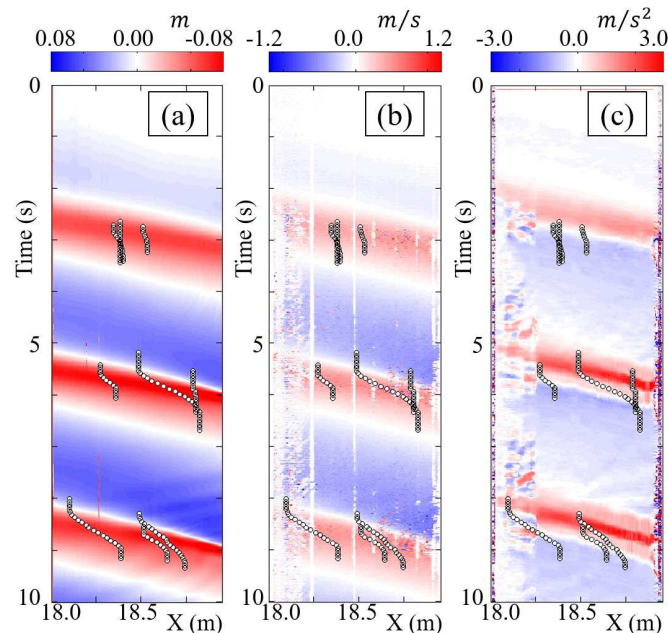


Figure 8. Temporal and spatial distributions of (a)water surface level, (b)velocity and (c)acceleration of near-bottom wave orbital current with tracks of representative moving gravels (blank circles) when periodic wave with period of 3sec was incident on the plane bed with slope of $\tan\beta=1/10$.

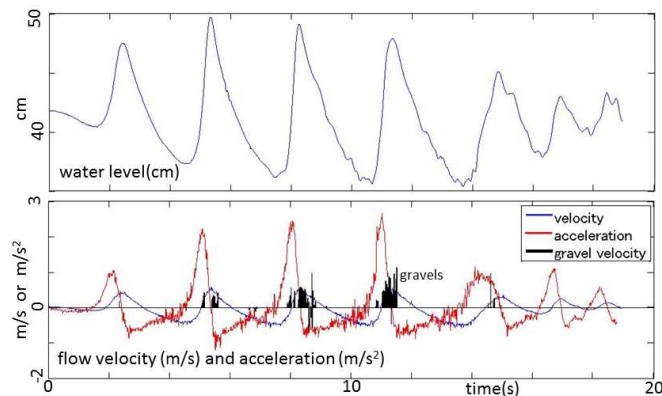


Figure 9. Time-profiles of water surface level (top), velocity and acceleration (bottom) of wave orbital current at $x=18.5\text{m}$, shown in Figure 8. Vertical bars indicate the velocity of each of moving gravels.

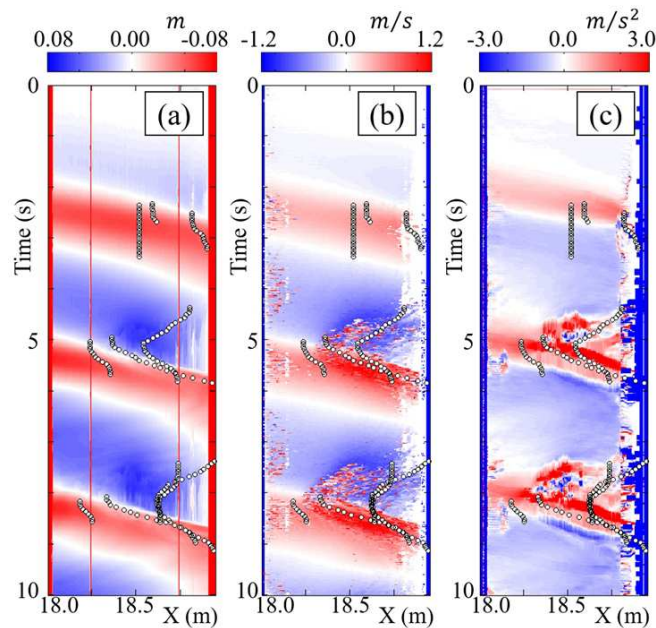


Figure 10. Temporal and spatial distributions of (a)water surface level, (b)velocity and (c)acceleration of near-bottom wave orbital current with tracks of representative moving gravels (blank circles) when periodic wave with period of 3sec was incident on the plane bed with slope of $\tan\beta=1/5$.

boundary of the figure, $h=22\text{cm}$, is the same as the one of Figure 8 but the water depth of Figure 10 becomes shallower and shallower with increasing x because the case of Figure 10 has the steeper bed slope. Observed horizontal velocity shown in Figure 10(b) is therefore relatively larger compared to the ones of Figure 8 and thus the overall velocity of moving gravels, which corresponds to the right downward slope of tracks, tend to be larger in the case of Figure 10. It should also be noted that Figure 10 also shows left downward tracks, which indicate offshoreward movement of gravels especially in the right half side of the figure, i.e., on the bed with shallower water depth.

While the peak onshoreward velocity of gravels tends to be larger in the case of Figure 10, the onshoreward velocity just after the initiation of onshoreward motion of gravels tend to be larger in the case of Figure 8 rather than those in Figure 10. Since both of shoreward velocity and acceleration appear to be larger in the case of Figure 10, this opposite trend may be due to the influence of steeper bed slope. Once gravels start to move, relative importance of this slope effect may decrease or deminish and the onshoreward velocity of gravels in Figure 10 dominates the one in Figure 8. Figure 10 also shows that two separate right downward tracks of gravels cross with each other, i.e., the one gravel behind the other gravel moves faster and eventually goes ahead of the other gravel. This feature should also be related to the relatively slower movement of gravels just after the initiation of onshoreward motion, which is dominantly observed in the case of steeper slope, i.e., Figure 10.

3.3. Behavior of Gravels in the Swash-zone

Figure 11(a) also shows temporal and spatial distributions of water surface level with tracks of moving gravels in the swash zone. The experimental case is the same as the one in Figure 10, i.e., the case with the uniformly sloping bed of $\tan\beta=1/5$. Figure 11(b) is the same as (a) zooming in the third wave and Figures 11(c) and 11(d) respectively show snap-shot images of wave runup and moving gravels at time, t_1 and t_2 , shown in Figure 11(b). In Figures 11(a) and (b), the area colored in monochromatic blue indicates that the bed level was higher than the instantaneous water level and thus the boundary of this monochromatic area corresponds to the time-varying instantaneous runup end.

In contrast to Figure 10, Figure 11 shows less offshoreward movement of gravels. This feature is consistent with observed equilibrium bed profile shown in Figure 3, in which the bed slope was steeper than $\tan\beta=1/5$ around the swash zone and thus onshoreward transport should be dominant on the slope of $\tan\beta=1/5$. While the slopes of right downward and left downward ends of runup and run down are about

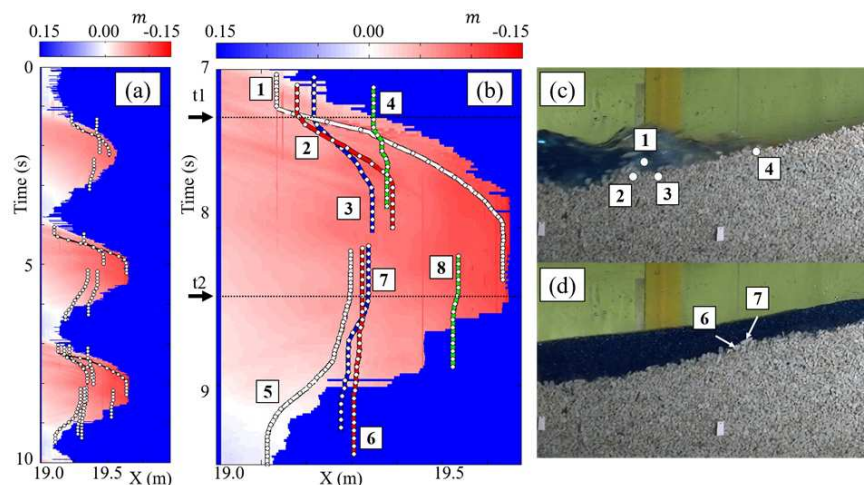


Figure 11. Temporal and spatial distributions of water surface level with tracks of moving gravels. Figure (a) covers first three waves, (b) zooms in the third wave, and (c) and (d) show snapshot images at time, t_1 and t_2 , indicated in (c). The identification number of gravels in (c) and (d) corresponds to the ones in (b).

the same, the onshoreward velocities of moving gravels were significantly larger than offshoreward velocities. Further analysis is needed for investigations of seepage effect on asymmetric wave orbital velocity fields and resulting asymmetric behavior of moving gravels.

Different onshoreward velocities of gravels, 1, 2, 3 and 4, may be explained by locations of each gravels shown in 11(c). The gravel 1, for instance, moves with faster velocity at the time, t_1 , and is located above the other gravels and appear to have less influence of the bottom slope. Similarly, different behaviors of gravels 6 and 7 may also be explained by slightly different locations of each gravel.

4. Summary and Conclusions

Laboratory experiments and image-based analysis were carried out to investigate the characteristic behavior of coral gravels under forward leaning waves around the surf and swash zones. Behavior of gravels was affected not only by near-bottom velocity but also by other factors such as acceleration of the fluid and bottom slopes. Especially around the swash zone, asymmetric onshoreward movement of gravels was enhanced and yielded locally steeper equilibrium bed slopes.

Acknowledgements

Authors acknowledges that a part of this research was funded by the Ministry of Land, Infrastructure, Transport and Tourism, Japan, and the University of Tokyo Ocean Alliance.

References

- Dean, R.G., 1965. Stream function representation of non-linear ocean waves, *Journal of Geophysical Research*, vol.70(18), pp.4561-4572.
- Fujikawa, H. and Tajima, Y., 2016. Experimental study on the formation of coral cays under waves and tides, *Journal of JSCE*, B2, vol.72, No.2, pp.I_553-I_558, doi: http://doi.org/10.2208/kaigan.72.I_553 (in Japanese).
- Kayanne, H., Aoki, K., Suzuki, T., et al., 2016. Eco-geomorphic processes that maintain a small coral reef island: Ballast Island in the Ryukyu Islands, Japan, *Geomorphology*, 271, pp.84-93.
- Tajima, Y., Liu, H. and Sato, S., 2009. Dynamic changes of waves and currents over the collapsing sandbar of the Tenryu river mouth observed during Typhoon T0704, *Proc. Coastal Dynamics 2009*, World Scientific.
- Takemori, R., Tajima, Y., Fujikawa, H. and Kayanne, 2015. Investigation on characteristics of local accumulation of coral gravels on an isolated reef, *Journal of JSCE*, B2 (Coast. Eng.), 71, No.2, pp.I_721-I_726 (in Japanese).